



HAL
open science

Improving the accuracy of the Jin-Xin relaxation scheme

Thierry Gallouët, Olivier Hurisse, Samuel Kokh

► **To cite this version:**

Thierry Gallouët, Olivier Hurisse, Samuel Kokh. Improving the accuracy of the Jin-Xin relaxation scheme. EDF R&D - dept. Mécanique des Fluides, Energies et Environnement. 2024. hal-04648134

HAL Id: hal-04648134

<https://hal.science/hal-04648134>

Submitted on 15 Jul 2024

HAL is a multi-disciplinary open access archive for the deposit and dissemination of scientific research documents, whether they are published or not. The documents may come from teaching and research institutions in France or abroad, or from public or private research centers.

L'archive ouverte pluridisciplinaire **HAL**, est destinée au dépôt et à la diffusion de documents scientifiques de niveau recherche, publiés ou non, émanant des établissements d'enseignement et de recherche français ou étrangers, des laboratoires publics ou privés.

Improving the accuracy of the Jin-Xin relaxation scheme.

T. Gallouët, O. Hurisse, S. Kokh

June 12, 2024

Contents

1	Introduction	1
2	Modifying the Jin-Xin relaxation scheme	2
2.1	The Jin-Xin relaxation approach	2
2.2	The Jin-Xin relaxation scheme	2
2.3	The GRU scheme for scalar advection	4
2.4	The modified Jin-Xin scheme	5
3	Numerical assessment of the modified scheme for Euler model	5
3.1	Comparison of computational efficiency	6
3.2	A pure contact-wave	6
3.3	A pure 3-shock wave	8
3.4	The SOD Riemann problem	8
3.5	Extended results for the SOD test case with different CFL numbers	9
3.6	Discussion on CPU efficiency for real EOS	14
4	Conclusion	16

1 Introduction

In industrial applications, the simulation of compressible flows often requires the use of complex Equations of State (EOS). From a computational point of view, the calls to the thermodynamic properties - which are mandatory in the algorithms - can become very costly in terms of CPU time. Algorithms that reduce the need to compute thermodynamic quantities through EOS are thus interesting for keeping the industrial simulations affordable. Moreover, several numerical schemes perform very well with simple analytical EOS but may have robustness issues when considering real EOS.

We focus here on simulations based on the Euler model, but the ideas developed remain quite general. When considering the Euler model, many relaxation procedures or methods have been proposed in the literature, see for instance [15, 7, 17, 2, 3]. All these schemes share the same principle, so let us briefly and roughly recall the idea of the Jin-Xin relaxation as proposed in [15] (it will be detailed in the paper). It should be noted that this scheme can be understood as an alternative way of writing the well-known Lax-Friedrichs scheme. In the Jin-Xin relaxation approach, a homogeneous non-linear system of conservation laws is approximated by a family of systems with a linear convection part and complemented by non-linear source terms which are parameterized by a small parameter ε . As ε goes to zero, the solutions of the relaxed system tend towards the solution of the non-linear system. From a numerical point of view, this parameter ε is not used and it is formally set to zero. Thanks to the form of the convective part of the relaxed system, the difficulties that could arise from the non-linearity of the convective part of the original system of equations are thus avoided. The convective part of the Jin-Xin relaxed model is then very easy to discretize since it relies on linear advection. More recent relaxation methods have been proposed [7, 17, 2, 3], for which fewer relaxed variables are used in order to limit numerical diffusion.

In the present work, a proposition is made in order to improve the accuracy of the Jin-Xin relaxation scheme. This scheme is composed of two steps: a first step in which scalar quantities corresponding to relaxed variables are advected, and a second step associated with a relaxation procedure that allows retrieving the original variables. Both steps introduce some numerical diffusion, but we focus here on the first one. The idea is to test the GRU projection step which has recently been proposed in [14, 11]. This algorithm is very simple and has interesting anti-diffusive properties. It is based on a random choice and is directly inspired from Glimm's ideas [12, 6] and from [9]. This first-order scheme is very well-suited for the advection of scalar quantities with discontinuities and can be applied to unstructured meshes. Several numerical tests [14, 11] have exhibited an effective convergence rate between 0.8 and 0.9 when considering problems of scalar advection with discontinuous profiles. Such profiles

are typically encountered in the first step of the Jin-Xin relaxation scheme.

The paper contains two sections. The first one describes the Jin-Xin relaxation scheme and the modifications for integrating the GRU step, while the second one presents some numerical comparisons and analysis based on three Riemann problems: a pure contact problem, a pure 3-shock problem, and the SOD test case. The results obtained with the Jin-Xin relaxation scheme with and without the GRU step are compared to the approximated solutions computed using the VRoe-ncv scheme using variables (U, P, s) . All tests were performed on a 1D computational domain and with perfect gas EOS, but the effect on efficiency of using real EOS is investigated.

2 Modifying the Jin-Xin relaxation scheme

2.1 The Jin-Xin relaxation approach

The Jin-Xin relaxation approach can be applied for a large class of systems of conservation laws. We focus here on its application to the Euler model:

$$\partial_t(W) + \partial_x(F(W)) = 0, \quad \text{with } W = (\rho, \rho U, \rho E), \quad F(W) = (\rho U, \rho U^2 + P, U(\rho E + P)), \quad (1)$$

where ρ stands for the density, U for the velocity, $E = e + U^2/2$ for the specific total energy, e for the specific internal energy, and $P = P(\rho, e)$ for the pressure law for which an EOS has to be given. The Jin-Xin relaxed model for system (1) reads:

$$\partial_t(W) + \partial_x(Y) = 0, \quad (2)$$

$$\partial_t(Y) + \Lambda \partial_x(W) = \frac{F(W) - Y}{\varepsilon}, \quad (3)$$

where $Y = (y_1, y_2, y_3)$ is the vector of the relaxed variables, $\varepsilon > 0$ is the relaxation parameter, and $\Lambda = \text{diag}(\lambda_1^2, \lambda_2^2, \lambda_3^2)$ is a 3×3 diagonal matrix with $\lambda_i \in \mathbb{R}$. **We insist here on the fact that the relaxation parameter ε is only used for the sake of building a Chapmann-Enskog expansion with respect to ε for regular solutions of system (2)-(3). The parameter ε is not used in a practical point of view and it is formally set to zero in the numerical scheme, see section 2.2 for details.**

The Chapmann-Enskog expansion of system (2)-(3) with respect to ε leads to:

$$\partial_t(W) + \partial_x(F(W)) = \varepsilon \partial_x((\Lambda - F(W)^2) \partial_x(W)). \quad (4)$$

This permits to highlight a stability constraint for system (2)-(3) which is a subcharacteristic condition. When Λ is such that:

$$\forall W, \quad (\Lambda - F(W)^2) > 0,$$

the operator on the right hand side of equation (4) corresponds to a diffusion operator that ensures the stability of the system.

It is an important point to be noted that the values λ_i do not depend on W nor Y , so that the convective system associated with (2)-(3) is linear. It can thus easily be recast in a diagonal form:

$$\partial_t(Z^+) + A \partial_x(Z^+) = G^+, \quad (5)$$

$$\partial_t(Z^-) - A \partial_x(Z^-) = G^-, \quad (6)$$

where $A = \text{diag}(\lambda_1, \lambda_2, \lambda_3)$, and where for all i we have:

$$W_i = Z_i^+ + Z_i^-, \quad Y_i = \lambda_i(Z_i^+ - Z_i^-), \quad \text{and} \quad G_i^\pm = \frac{1}{\varepsilon} \left(\frac{1}{2} \left(\frac{F_i(W)}{\lambda_i} \pm W \right) - Z_i^\pm \right).$$

In system (5)-(6) the convective part of the equations are linear and decoupled. This system is the used for computing approximated solutions of system (1).

2.2 The Jin-Xin relaxation scheme

Let us now describe the numerical strategy retained for computing approximate solution of system (1) through Jin-Xin relaxed system (5)-(6). It relies on a first-order Lie-Trotter splitting that successively:

- handles the convection part using a first-order finite-volume scheme,
- and account for the stiff relaxation of the source terms for $\varepsilon \rightarrow 0$.

It should be noted that more complex strategies have been proposed, based on high order splitting and schemes, as for instance in [8, 1]. The strategy followed here differs since we intend to be able to apply easily the method to 2D/3D configurations with non structured meshes.

Let us assume that the approximated solution is known at time t^n on a regular mesh with a size Δx . The approximated value of W_i , Y_i and Z_i^\pm in cell j at time t^n is denoted respectively by $W_{i,j}^n$, $Y_{i,j}^n$ and $(Z_{i,j}^\pm)^n$. The time-step at iteration n is Δt^n and it is chosen according to a CFL constraint arising in the convection step (see below).

Convection step: $t^n \rightarrow t^*$.

We choose here to discretize the convective part of the system by using the basic Upwind scheme which simply reads here:

$$(Z_{i,j}^+)^* = (Z_{i,j}^+)^n - \lambda^n \frac{\Delta t^n}{\Delta x} \left((Z_{i,j}^+)^n - (Z_{i,j-1}^+)^n \right), \quad (7)$$

$$(Z_{i,j}^-)^* = (Z_{i,j}^-)^n + \lambda^n \frac{\Delta t^n}{\Delta x} \left((Z_{i,j+1}^-)^n - (Z_{i,j}^-)^n \right). \quad (8)$$

The value λ^n is computed at each time-step and it reads:

$$\lambda^n = a \times \max_j (|U_j^n| + c_j^n),$$

where $a > 1$ and where c_j^n is the sound speed computed in cell j at iteration n . Since the parameter a is directly involved in the diffusion coefficient on the right hand side of equation (4), the numerical diffusion of the scheme increases when a increases. The classical CFL constraint for the time-step Δt with Upwind scheme is:

$$\Delta t^n \leq \frac{\Delta x}{\lambda^n}. \quad (9)$$

With this constraint, the convection scheme is monotonicity preserving for the relaxed variables Z_i^\pm . This is an important feature for the modification proposed in this work.

Relaxation step: $t^* \rightarrow t^{n+1}$.

This step accounts for the relaxation term source G^\pm in system (5)-(6). Since it is a cell-wise update, cell subscript are omitted here. The set of equations used here are thus:

$$\partial_t (Z^+) = G^+, \quad (10)$$

$$\partial_t (Z^-) = G^-, \quad (11)$$

with initial condition $Z^+(t=0) = (Z^+)^*$ and $Z^-(t=0) = (Z^-)^*$. We impose here an instantaneous relaxation which corresponds to setting $\varepsilon \rightarrow 0$ in (10)-(11) and to solve the non-linear problem:

$$\frac{1}{2} \left(\frac{F_i(W)}{\lambda_i} \pm W \right) - Z_i^\pm = 0.$$

In these equations, the terms depending on W are computed explicitly with $(Z^\pm)^*$ and the last term on the left hand side is set to $(Z_i^\pm)^{n+1}$:

$$(Z_i^\pm)^{n+1} = \frac{1}{2} \left(\frac{F_i(W^*)}{\lambda_i^n} \pm W^* \right).$$

For the Euler model, the update procedure for this relaxation step then reads:

(i) Computation of the conservative variables W_i^* :

$$\rho^* = (Z_1^+)^* + (Z_1^-)^*, \quad (12)$$

$$(\rho U)^* = (Z_2^+)^* + (Z_2^-)^*, \quad (13)$$

$$(\rho E)^* = (Z_3^+)^* + (Z_3^-)^*. \quad (14)$$

$$(15)$$

(ii) Computation of the fluxes $F_i^* = F_i(W^*)$:

$$U^* = (\rho U)^* / \rho^*, \quad (16)$$

$$P^* = P(\rho^*, (\rho E)^* / \rho^* - (U^*)^2 / 2), \quad (17)$$

$$F_1^* = (\rho U)^*, \quad (18)$$

$$F_2^* = (\rho U)^* U^* + P^*, \quad (19)$$

$$F_3^* = U^* ((\rho E)^* + P^*). \quad (20)$$

$$(21)$$

(ii) Computation of the updated relaxed variable $(Z_i^\pm)^{n+1}$:

$$(Z_1^-)^{n+1} = (-F_1^*/\lambda_1^n + \rho^*)/2, \quad (22)$$

$$(Z_1^+)^{n+1} = (F_1^*/\lambda_1^n + \rho^*)/2, \quad (23)$$

$$(Z_2^-)^{n+1} = (-F_2^*/\lambda_2^n + (\rho U)^*)/2, \quad (24)$$

$$(Z_2^+)^{n+1} = (F_2^*/\lambda_2^n + (\rho U)^*)/2, \quad (25)$$

$$(Z_3^-)^{n+1} = (-F_3^*/\lambda_3^n + (\rho E)^*)/2, \quad (26)$$

$$(Z_3^+)^{n+1} = (F_3^*/\lambda_3^n + (\rho E)^*)/2. \quad (27)$$

$$(28)$$

It should be remarked that, per time-step and per cell, only 2 calls to thermodynamical functions are required for the whole algorithm. One is needed for computing the pressure and one for computing the sound speed. This is less than most of the approximate Godunov solvers. This low number of thermodynamical calls is a key point for explaining the efficiency of this scheme in terms of CPU-time. It should be noted that the Jin-Xin scheme can be seen as an alternative way of writing the Lax-Friedrichs scheme.

2.3 The GRU scheme for scalar advection

It has been seen in section 2.2 that the convective step of the scheme is based on linear scalar advection. Recently, an efficient stochastic scheme for scalar advection has been proposed in [11]. It is nicknamed GRU and it relies on the same kind of idea than the Glimm's scheme [12]. Unlike the latter, the GRU scheme [11] can be applied to 2D or 3D configurations including unstructured meshes, but it is restricted to scalar advection (linear and non-linear). In this section, the GRU scheme for linear advection is presented.

We assume here that the quantity $\phi(t, x)$ is advected with velocity V , which is positive and which does not depend on space and time:

$$\partial_t(\phi) + V\partial_x(\phi) = 0. \quad (29)$$

For computing approximated solutions of this equation, a fractional step approach is used. The first step is a convection step, which can be seen as a prediction step. It is assumed that the approximated solutions are computed thanks to the Upwind scheme. The approximated values in cell i obtained from the sequence (ϕ_i^n) of the approximated solution at iteration n through the Upwind scheme are:

$$\phi_i^{n,*} = (1 - \beta_i^n)\phi_i^n + \beta_i^n\phi_{i-1}^n.$$

The parameter $\beta_i^n = V\Delta t^n/\Delta x_i$ has to be smaller than 1 in order to ensure the stability of the Upwind scheme. Then the GRU step is applied in each cell on the basis of the predicted value $\phi_i^{n,*}$. For that purpose, we consider a random number ω^n that follows a uniform distribution in $[0, 1]$. The GRU step simply reads:

$$\phi_i^{n+1} = \begin{cases} \phi_{i,m}^n, & \text{if } \phi_i^{n,*} < \omega_i^n, \\ \phi_{i,M}^n, & \text{otherwise;} \end{cases} \quad (30)$$

where $\phi_{i,m}^n$ and $\phi_{i,M}^n$ are respectively the local minimum and the local maximum of the cell values at time t^n when considering the set of the upwind cells with respect to the mass fluxes. Since we have here $V > 0$, we get: $\phi_{i,m}^n = \min(\phi_{i-1}^n, \phi_i^n)$ and $\phi_{i,M}^n = \max(\phi_{i-1}^n, \phi_i^n)$. The number ω_i^n is a renormalization of the number ω^n over $[\phi_{i,m}^n, \phi_{i,M}^n]$:

$$\omega_i^n = \phi_{i,m}^n + \omega^n(\phi_{i,M}^n - \phi_{i,m}^n), \quad (31)$$

so that ω_i^n follows the uniform distribution on $[\phi_{i,m}^n, \phi_{i,M}^n]$. An important point to be quoted here is that the same ω^n is used for all the cells. This is a cornerstone of such algorithms, as noticed in [4, 5] for the Glimm's scheme. In a practical point of view, ω^n is chosen in low-discrepancy sequences with values in $[0, 1]$. They are well-suited for the Glimm's scheme [4, 16, 6] as well as for the GRU step [14, 11].

Despite its simplicity, this scheme has very interesting properties for approximating weak solutions of (29) [14, 11]. Discontinuities are maintained perfectly sharp and no intermediate values are created by the scheme. The scheme is not conservative and the approximated discontinuities may not be located at the exact position. Nevertheless, for a simple configuration, it has been proved that the approximated solutions computed with the Upwind scheme and the GRU step converge with order 1 in probability [10] (convergence almost surely can also be proved). In a practical point of view, using low-discrepancy sequences as pseudo-random generators, effective convergence rates between 0.8 and 0.9 have been obtained for a wide range of problems involving discontinuities in 1D and 2D with unstructured meshes. For all these test cases, the GRU step largely improved the accuracy of the Upwind scheme.

2.4 The modified Jin-Xin scheme

The idea proposed in this work is to test the GRU step of section 2.3 for the advection step (5)-(6) in the Jin-Xin relaxation scheme. The scheme denoted by Jin-Xin-GRU in this work is thus the 3-step scheme defined by the following steps:

- 1 - the convection step of the Jin-Xin relaxation scheme described in section 2.2;
- 2 - the GRU projection step of section 2.3 applied to the relaxed variables $(Z_i^\pm)^*$ and defined by (30);
- 3 - the relaxation step of the Jin-Xin relaxation scheme described in section 2.2.

The main idea here is to get rid of the numerical diffusion in the advection step of the Xin-Jin scheme and to gain accuracy on the approximated solutions computed by the whole scheme. Some numerical tests are thus carried out in the next section in order to assess whether the improvement is significant or not. It should be noticed that even if the GRU step limits the numerical diffusion in the advection of the relaxed variables, the computation of the conservative variables in the Jin-Xin relaxation step (12)-(14) causes some numerical diffusion.

3 Numerical assessment of the modified scheme for Euler model

In this section, different numerical tests are performed on the basis of several exact solutions of Riemann problems for system of equations (1): a pure contact case (see section 3.2), a pure shock case (see section 3.3) and the SOD test case (see section 3.4). All these test cases are defined for $x \in [0, 1]$ and the initial discontinuity in the definition of the Riemann problems is located at $x = 1/2$. The left state (resp. right state), denoted by L (resp. R), defines the initial condition for $x < 1/2$ (resp. for $x > 1/2$).

We focus on the perfect gas pressure law: $P(\rho, e) = (\gamma - 1)\rho e$ with $\gamma = 1.4$ and we restrict to 1D domain with regular meshes. The approximated solutions will be computed with three different schemes: the Jin-Xin relaxation of section 2.2, the Jin-Xin-GRU 3-step scheme defined in section 2.4, and the VFRoe-cv scheme using the variable (U, P, s) (for entropy-velocity-pressure) CITE. The latter is an accurate approximate Godunov solver whose numerical fluxes are computed using the exact solution of a Riemann problem based on a linearized Euler system.

For the Jin-Xin and Jin-Xin-GRU relaxation schemes, the parameter a defined in section 2.2 - and related to the convection step - is set to 1.0001 and we define:

$$\Delta t_{lim}^n = \frac{\Delta x}{\lambda^n}. \quad (32)$$

The CFL constraint (9) then reads: $\Delta t^n \leq \Delta t_{lim}^n$. The time-step at iteration n can be written: $\Delta t^n = C_{cfl} \Delta t_{lim}^n$ with the CFL parameter C_{cfl} in $[0, 1]$. A sufficient condition for the VFRoe-ncv scheme to provide stable approximations is to have a CFL parameter lower than 0.5. It should be noted that CFL numbers between 0.5 and 1 can usually be used, but approximate solutions may become unstable for some severe test cases. In order to perform comparisons between the three schemes, we consider in sections 3.2, 3.3 and 3.4 the CFL parameter $C_{cfl} = 0.45$. Since a is very close to 1, the numerical diffusion in the Jin-Xin convection step is low and strongly depends on C_{cfl} . It should be noted that approximated solutions obtained with the Jin-Xin and Jin-Xin-GRU schemes for higher CFL parameters will be examined in section 3.5.

Some convergence curves will be discussed for the test cases with the help of the L^1 -relative error:

$$\text{err}_1((\psi_i^n)_i) = \frac{\sum_i |\psi_i^n - \psi^{ex}(t^n, x_i)|}{\sum_i |\psi^{ex}(t^n, x_i)|},$$

where ψ denotes the density, the velocity or the pressure; and where $(\psi_i^n)_i$ is the approximated solution computed at iteration n and $\psi^{ex}(t^n, x_i)$ is the value of the exact solution a time t^n and at the center x_i of cell i .

At last, the uniform law in the GRU step is replaced by a low-discrepancy sequence. If several choices are possible and have been tested for the GRU step in [14, 11], we restrict here to a sole sequence generated thanks to the linear congruential generator defined by:

$$\omega^{k+1} = \text{rem} \left(\omega^k + \frac{\sqrt{5}-1}{2}, 1 \right),$$

with the initial value $\omega^0 = 0.05$, and where $\text{rem}(x, y)$ is the remainder of the division of x by y .

3.1 Comparison of computational efficiency

As mentioned in section 2.3, the expected computational time per iteration and per cell is expected to be less for the Xin-Jin and Xin-Jin-GRU relaxation schemes than for the VFRoe-ncv scheme. Let us define for each scheme \mathcal{S} the function $\Delta x \rightarrow \text{CPU}_{\mathcal{S}}(\Delta x)$ that represents the computational time needed for a given simulation (for given initial conditions, given CFL parameter, given final time, and given EOS parameter) with a mesh size Δx . The three schemes are respectively denoted by $\mathcal{S} = \{vf, jx, jxg\}$ for the VFRoe-ncv scheme, for the Jin-Xin relaxation scheme and for the Jin-Xin-GRU relaxation scheme. As usual for first-order finite-volumes scheme, we have for all schemes \mathcal{S} and for all $\alpha > 0$:

$$\text{CPU}_{\mathcal{S}}(\alpha\Delta x) = \left(\frac{1}{\alpha}\right)^2 \text{CPU}_{\mathcal{S}}(\Delta x). \quad (33)$$

This law has been checked for our three schemes. Moreover, the following relations have been obtained:

$$\text{CPU}_{vf}(\Delta x) \sim 3 \times \text{CPU}_{jx}(\Delta x), \quad (34)$$

$$\text{CPU}_{vf}(\Delta x) \sim 2 \times \text{CPU}_{jxg}(\Delta x). \quad (35)$$

In other words, for a given simulation, VFRoe-ncv scheme costs 3 times more than the Jin-Xin scheme and 2 times more than the Jin-Xin-GRU scheme. Let us assume that a simulation is performed with the VFRoe-ncv scheme for a given mesh size Δx . For the same configuration, the mesh size $\alpha\Delta x$ to be used with the Jin-Xin relaxation scheme in order to get the same CPU time is then obtained thanks to relations (33)-(34):

$$\begin{aligned} \text{CPU}_{jx}(\alpha\Delta x) &= \text{CPU}_{vf}(\Delta x) \\ \stackrel{\text{eq. (33)}}{\iff} \left(\frac{1}{\alpha}\right)^2 \text{CPU}_{jx}(\Delta x) &= \text{CPU}_{vf}(\Delta x) \\ \stackrel{\text{eq. (34)}}{\iff} \left(\frac{1}{\alpha}\right)^2 \frac{1}{3} \text{CPU}_{vf}(\Delta x) &= \text{CPU}_{vf}(\Delta x) \\ \iff \alpha &= \sqrt{\frac{1}{3}} \end{aligned}$$

We thus get $\alpha \sim 0.58$. The same computation can be done for the Jin-Xin-GRU scheme and it gives:

$$\alpha = \sqrt{1/2} \sim 0.71.$$

These two quantities are useful since they allow to modify a convergence curve giving the error with respect to the mesh size into a curve that allows to compare the error with respect to the CPU time, which is also a very important information for practical applications. This will be used in the following sections.

We conclude this section by adding few remarks on the memory consumption for the different numerical schemes. The VFRoe-ncv scheme and the Xin-Jin relaxation schemes (with or without GRU step) are different in term of memory management. Indeed, the two relaxation schemes require 2 times more memory storage for the relaxed variables (the conservative variable is not stored), but there is no interfacial flux to be stored. On the contrary, for the VFRoe-ncv scheme memory is needed for the set of conservative variables and for the interfacial fluxes. The three schemes then require the same amount of memory. It should be noted that it is possible not to store the interfacial fluxes for the VFRoe-ncv scheme. But in this case, each one will be computed twice, which roughly multiply the CPU time by two. In fact, the three schemes are not significantly different in terms of memory storage and the choice between relaxation scheme and VFRoe-ncv should be made based on the computer architecture (GPU, CPU, ...), on the amount of memory available and on the latency in memory access.

3.2 A pure contact-wave

For this test case, the initial conditions of the Riemann problem are given in figure 1. The exact solution is such that the pressure and the velocity are constant and uniform: $P(t, x) = 10^5$ and $U(t, x) = 50$; and the initial density profile is advected with velocity U , that is: $\rho(t, x) = \rho(0, x - 50 t)$. The two GNL waves are ghost waves.

With the three schemes P and U are maintained uniform and constant without any spurious oscillations as in many first-order explicit schemes. On the contrary, the density profile strongly differs. The amount of numerical diffusion on the contact wave is clearly highlighted by this test case. The three density profiles are plotted in figure 2 at time $t = 6 \cdot 10^{-4} s$ for a mesh with 1024 cells. For a given mesh size, it clearly appears that the two relaxation schemes lead to more numerical diffusion than the VFRoe-ncv scheme. The GRU step slightly lowers the numerical diffusion for the Jin-Xin scheme. Convergence curves are plotted in figure 3 with respect to the mesh size and with respect to the CPU time, according to relations of section 3.1 (curves have been shifted by $\log(1/\alpha)$ on the x-axis). It can clearly be observed that the VFRoe-ncv scheme gives better approximations for the density. For the pressure and velocity profiles all the schemes provide the same error for a given mesh size. Therefore, for a given CPU-time the relaxation schemes have a small advantage.

	L	R
ρ (kg/m^3)	1	0.125
U (m/s)	50	50
P (Pa)	10^5	10^5

Figure 1: Initial conditions for the Riemann problem consisting in a pure contact wave.

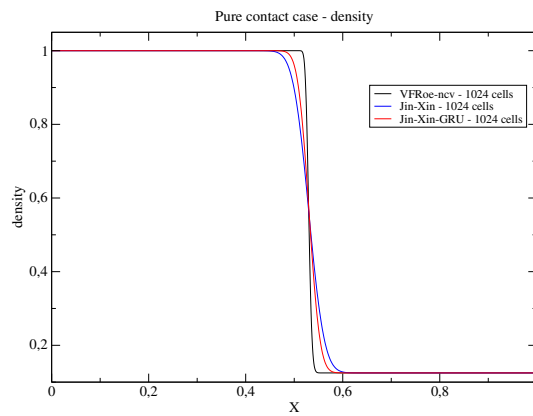


Figure 2: Pure contact wave test case: approximated density profiles for a mesh with 1024 cells.

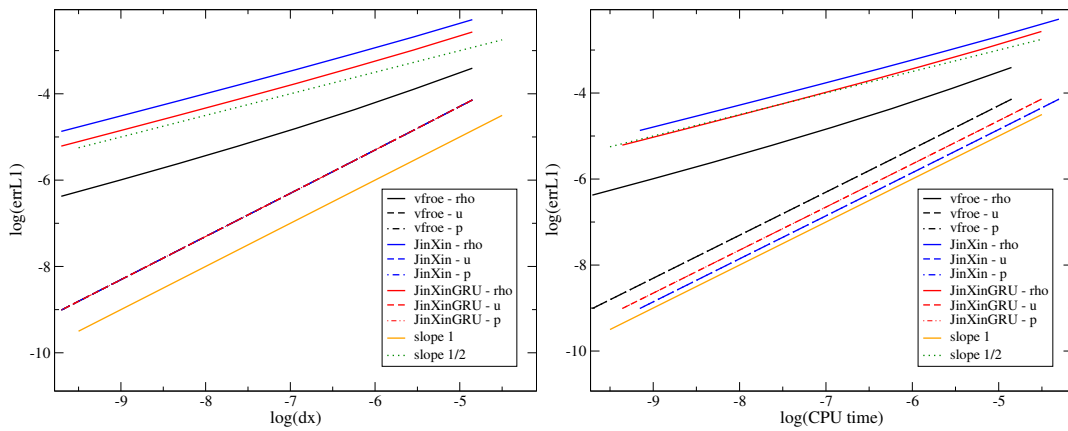


Figure 3: Pure contact wave test case: convergence curves for the three schemes with respect to the mesh size (left figure) and to the CPU-time (right figure). Meshes contain from 128 up to 16384 cells.

	L	R
ρ (kg/m^3)	1	0.5
U (m/s)	0	$-100 \times \sqrt{\frac{70}{11}}$
P (Pa)	10^5	$\frac{4}{11} \times 10^5$

Figure 4: Initial conditions for the Riemann problem consisting in a pure contact wave.

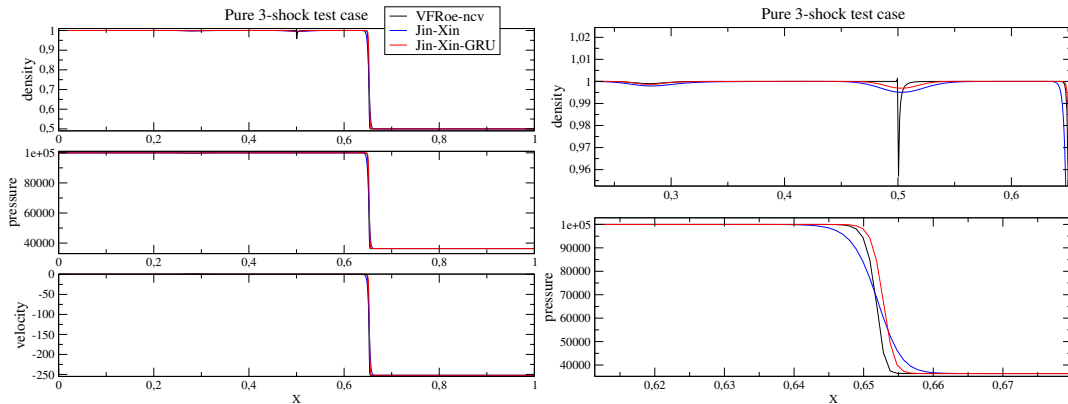


Figure 5: Pure 3-shock wave test case: approximated profiles for the Riemann problem consisting in a pure 3-shock wave, the mesh contains 1024 cells. On the left the whole domain, on the right zoom on the pressure and density profiles.

3.3 A pure 3-shock wave

We consider here a Riemann problem that generates a single 3-shock wave. Left and right states are given in figure 4 and the 3-shock travels to the right with a speed $\sigma \sim 252$ m/s . The contact wave and the 1-wave are ghost waves. It should be noted that the contact wave is steady since the intermediate velocity in the associated Riemann problem is equal to zero (i.e. the velocity between the the GNL waves is uniform and constant equal to zero).

The approximated solutions computed with the three schemes have been plotted in figure 5 at time $t = 6 \cdot 10^{-4}$ s for a mesh with 1024 cells: on the left the density, pressure and velocity have been plotted on the whole domain, while a zoom is proposed in the figure on the right. In the latter, both density and pressure have been plotted. The zoom on the density profile highlights that undershoots appear in the approximated solutions around the contact wave position ($x = 0$) and around the location of the 1-wave ($x \sim 0.27$). These undershoots tend to vanish when the mesh is refined. Moreover, the zoom on the pressure profile allows to appreciate the stiffness of the approximated shock. In particular, one can observe that the GRU step permits to recover a shock profile which is as stiff as the shock profile computed by the VFRoe-ncv scheme. It can also be remarked that the location of the approximated shock seems to be different for the Jin-Xin-GRU scheme. This is due to the GRU step and to the random choice. In fact, for the Jin-Xin-GRU scheme, the approximated shock is not located at the correct location even if it converges to the exact position when the mesh is refined. This can be seen on the convergence curves in figure 6. All the variables converge with order 1, which means that the undershoots located at the contact location on the density profiles tends to vanish with order 1. This would probably be different for a more complex EOS (see CITE contact). The most important remarks for this test case are the following.

- For a given mesh, the VFRoe-ncv scheme is more accurate than the two relaxation schemes for all the variables. The GRU step seems to slightly improve the accuracy for the velocity and the pressure. In particular, the shock profile is more accurate despite it is not exactly at the good location. Moreover, the undershoots at the ghost wave locations are reduced by using the GRU step. Nevertheless, the random choice involved in the GRU step introduces some small oscillations in the profiles.
- For a given CPU-time, the three schemes give very close results, with a tiny advantage for the Jin-Xin scheme without GRU step.

3.4 The SOD Riemann problem

The classical SOD Riemann problem is considered here, the initial conditions of which are recalled in figure 7. The solution of SOD problem involves a 1-rarefaction wave that travels to the left, a right going contact wave, and a 3-shock wave that propagates to the right of the domain. It should be noted that the right side of the fan of the

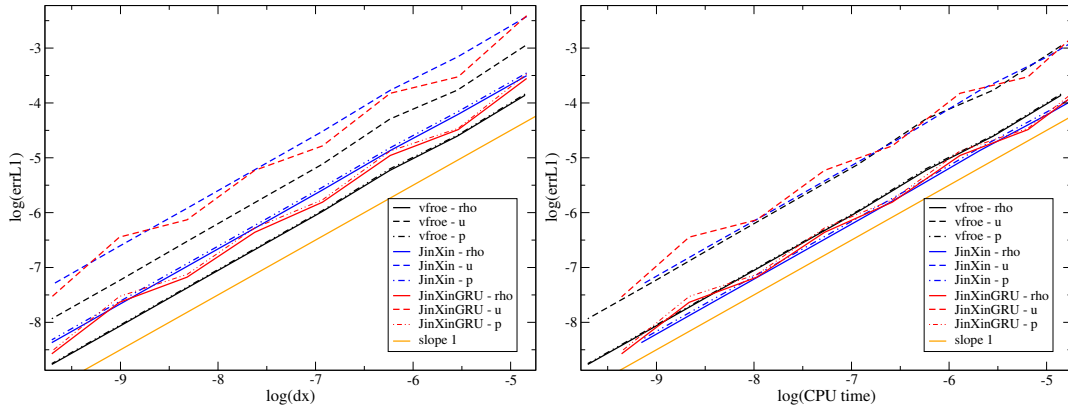


Figure 6: Pure 3-choc wave test case: convergence curves for the three schemes with respect to the mesh size (left figure) and to the CPU-time (right figure). Meshes contain from 128 up to 16384 cells.

	L	R
ρ (kg/m^3)	1	0.125
U (m/s)	0	0
P (Pa)	10^5	10^4

Figure 7: Initial conditions for the SOD Riemann problem.

1-rarefaction travels very slowly to the left with respect to the speed of the other waves.

The three approximated solutions obtained with the three schemes for a mesh with 1024 cells are plotted in figure 8. The left part in figure 8 corresponds to a view over the whole domain, whereas the right one gathers: a zoom on the contact wave for the density profile, a zoom on the pressure intermediate state (between the right part of the fan of the 1-rarefaction and the 3-shock), and a zoom on the shock for the velocity profile. As for the test case 3.2 and 3.3, the GRU step improves the accuracy of the contact and the stiffness of the shock profile. These improvements are a little bit more important because of the time-step (32) which is optimal for the shock here. Indeed, in SOD test case the time-step is computed on the basis of the speed of the shock wave which is the fastest wave. In the problem of section 3.3 the fastest wave is the 1-rarefaction wave, even if it is a ghost wave. The time-step is thus not optimal for the 3-shock in the problem of section 3.3. Moreover, the contact wave has a speed which is important more important in SOD problem than in the problem of section 3.2. Therefore, the time-step chosen with respect to the shock wave leads here to more accuracy for the contact wave. The zoom on the pressure profiles clearly exhibits oscillations that directly arise from the random choice in the GRU step. The GRU step combined to the convection step make the profiles of the relaxed variables jump to the left or the right depending on the random number. When the conservative variables are built from these relaxed variables in the relaxation step, oscillations appear.

The convergence curves are plotted in figure 9. For this test case, the improvement of the GRU step is more important than for the two previous ones. For a given mesh size, the accuracy is improved with respect to the Jin-Xin relaxation scheme; and for a give CPU-time the Jin-Xin-GRU scheme is as accurate as the VFRoe-ncv scheme. In fact, for the present test case, the time-step is optimal for the shock and there is only two or three points in the shock profile computed by the Jin-Xin-GRU scheme whatever the mesh size is, see figure 10. Nevertheless, as for the test case of section 3.3 the approximated shock is not located at the location of the exact shock, even if it tends towards the exact ones when mesh is refined. With respect to the VFRoe-ncv scheme, the error in the computation of the approximated solution with the Jin-Xin-GRU scheme arises from the location of the shock and in the oscillations introduced in the intermediate states (between the rarefaction wave and the shock wave).

3.5 Extended results for the SOD test case with different CFL numbers

Up to now we focused on regular meshes and a CFL number of 0.45. In the present section, some comparisons are proposed on the basis of the SOD test case of section 3.4. As it has been mentioned in the introduction of section 3, CFL numbers between 0.5 and 1.0 can be used for many test cases and the limitation to CFL numbers less than 0.5 is mandatory only for some severe test cases. For instance, the VFRoe-ncv scheme can be applied up to a CFL number of 0.95 with the SOD test case of section 3.4. So that, using a CFL number of 0.45 is in general a matter of caution for VFRoe-ncv scheme. Hence, even if more accurate approximations could be obtained here with the VFRoe-ncv scheme by using higher CFL numbers, the results for $CFL = 0.45$ are considered as the references.

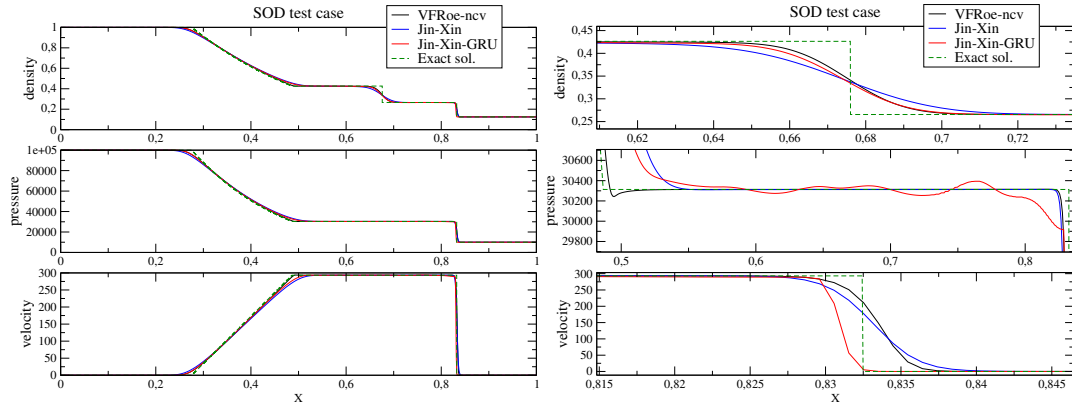


Figure 8: SOD test case: approximated profiles for the SOD Riemann problem, the mesh contains 1024 cells. On the left the whole domain, on the right zoom on the pressure and density profiles.

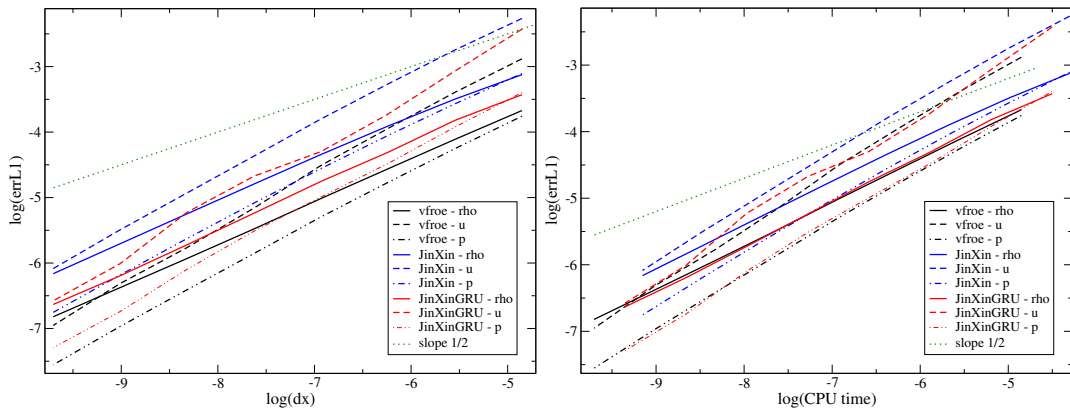


Figure 9: SOD test case: convergence curves for the three schemes with respect to the mesh size (left figure) and to the CPU-time (right figure). Meshes contain from 128 up to 16384 cells.

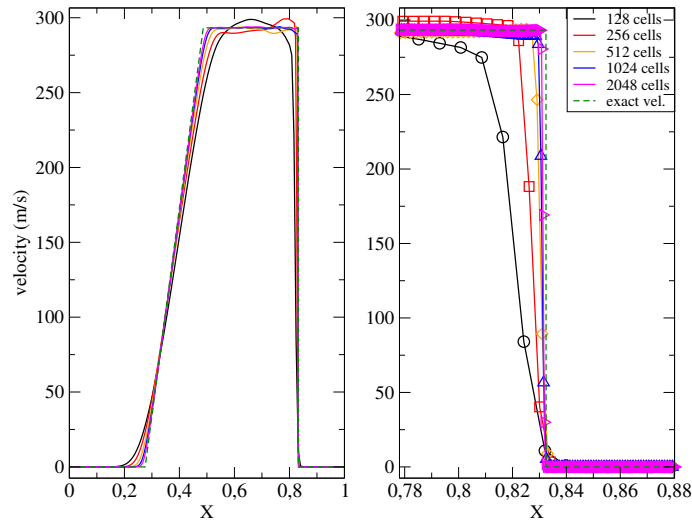


Figure 10: SOD test case for the Jin-Xin-GRU relaxation scheme: shock wave on the approximated velocity profile for different uniform meshes. For all the meshes the approximated shock profile contains two or three cells.

We focus here on the fact that the two relaxation schemes allow to reach a CFL number close to 1.0 whatever the test cases. In terms of CPU-time this is an important feature since for a given test case with a given final time, the CPU-time is linear with respect to the CFL number. In other words, the computations require 2 time less iterations at CFL 1.0 than at CFL 0.5. The CPU time is thus 2 times less, increasing the advantage of the relaxation scheme over the VFRoe-ncv scheme for the SOD test case when considering the error versus the CPU-time. For the VFRoe-ncv scheme $C_{cfl} = 0.475$ is chosen and for the Jin-Xin relaxation schemes we set the CFL to: $C_{cfl} = 2 \times 0.475 = 0.95$. With these choices, relations (34) and (35) which were proposed for equal CFL numbers become here:

$$\text{CPU}_{vf}(\Delta x) \sim 2 \times 3 \times \text{CPU}_{jx}(\Delta x), \quad (36)$$

$$\text{CPU}_{vf}(\Delta x) \sim 2 \times 2 \times \text{CPU}_{jxg}(\Delta x). \quad (37)$$

We first compare the approximated solutions computed by the sole relaxation schemes for a mesh with 1024 cells and for different CFL number $C_{cfl} = \{0.15, 0.3, 0.45, 0.60, 0.75, 0.9\}$. The error with respect to the CFL number is plotted in figure 11. The error with respect to the CFL number is a decreasing function of the CFL number for the Jin-Xin scheme. With the GRU step, the error is constant for $C_{cfl} < 1/2$ and an increasing function for $C_{cfl} > 1/2$. Both errors become almost equal for the higher CFL numbers. The same behavior has been observed with Halton-Van der Corput low-discrepancy sequences. Approximated solutions for the density have been plotted in figure 12 for a CFL number of 0.9 and 0.15. From figure 12, it can be observed that the rarefaction wave and the contact wave are not improved by increasing the CFL number with the GRU step, whereas they are improved without. The accuracy on the shock wave is better for large CFL numbers without the GRU step.

Since the GRU step increases the CPU-time of the Jin-Xin relaxation scheme by 50%, the results above tend to show that the GRU step does not improve the Jin-Xin relaxation scheme on uniform meshes, at least when considering CFL number close to 1.0. Nevertheless, for non-uniform meshes, the time-step Δt^n is chosen accordingly to the most penalizing cell. For the other cells, this time step can be associated with a (very) low local CFL number. Therefore, the improvement of the GRU step for the small CFL number, i.e. roughly speaking for the larger cells, could be interesting. Let us compare the approximated solutions computed using the Jin-Xin relaxation schemes and the VFRoe-ncv scheme for the SOD test case and non-uniform meshes. We use here a mesh whose cell size is given by a sinusoidal function with a period of $0.2 m$ and a ratio of 10 between largest and smallest cell sizes. Convergence curves are plotted in figure 13 with the modified L^1 -relative error:

$$\text{err}_1((\psi_i^n)_i) = \frac{\sum_i (\Delta x_i |\psi_i^n - \psi^{ex}(t^n, x_i)|)}{\sum_i (\Delta x_i |\psi^{ex}(t^n, x_i)|)},$$

where Δx_i is the size of cell i . In figure 13 the reference mesh size for plotting the error versus mesh size is the minimum of the size of the cells:

$$\Delta_x^m = \min_j (\Delta x_j).$$

The time-step limit (32) now reads:

$$\Delta t_{lim}^n = \frac{\Delta_x^m}{\lambda^n}. \quad (38)$$

The CFL numbers 0.475 and 0.95 used here are defined here with respect to the time-step limit (38). The approximated density profiles obtained for three meshes are compared in figure 14. It clearly appears in this figure that for this test case the GRU step improves the accuracy of the Jin-Xin relaxation scheme for the three waves (1-rarefaction, contact and 3-shock). The gain in terms of accuracy when using the GRU step is large enough to compensate for the 50% higher CPU time induced by the GRU step at a given mesh size. The improvement seems particularly important for the shock. Moreover, in terms of CPU efficiency, the Jin-Xin-GRU scheme has clearly a small advantage over the VFRoe-ncv scheme.

Remark. For CFL numbers above 1, the Jin-Xin relaxation scheme and the VFRoe-ncv scheme are unstable whereas the Jin-Xin-GRU scheme remains stable. This is due to the fact that the instabilities arising in the convection step are filtered by the GRU step (projection step). Nevertheless, it should be noted that even if it remains stable, the Jin-Xin-GRU is no more consistent for $C_{cfl} > 1$. This is due to the statistical consistency of the GRU step that requires a convection step which preserves monotonicity (otherwise statistical bias are introduced and consistency is lost), see [14, 10, 11]. Density profiles for different CFL numbers greater than 1 have been plotted in figure 15.

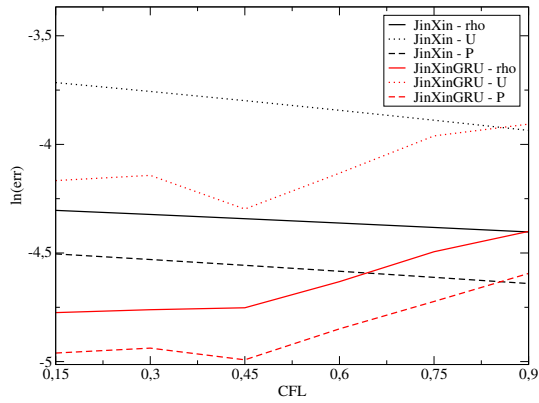


Figure 11: SOD test case: error with respect to the CFL number for a mesh with 1024 cells.

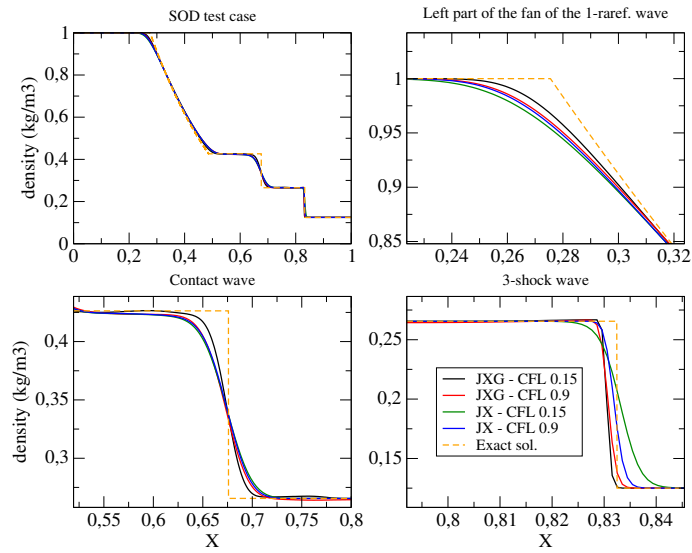


Figure 12: SOD test case: comparison of the approximated solutions for CFL numbers 0.15 and 0.9 for a mesh with 1024 cells.

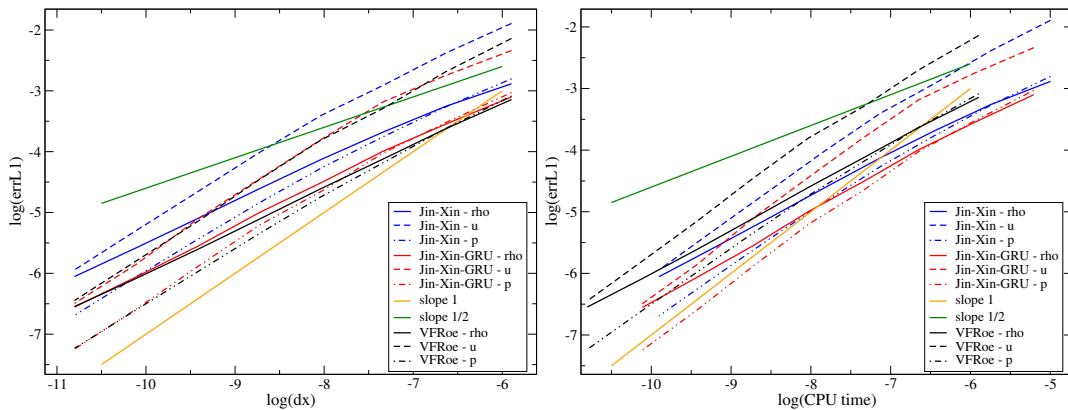


Figure 13: SOD test case: convergence curves for the three schemes with respect to the mesh size (left figure) and to the CPU-time (right figure). Meshes are non-uniform and contain from 128 up to 16384 cells. For the VFRoe scheme the CFL is equal to 0.475, and for the relaxation schemes the CFL is equal to 0.95.

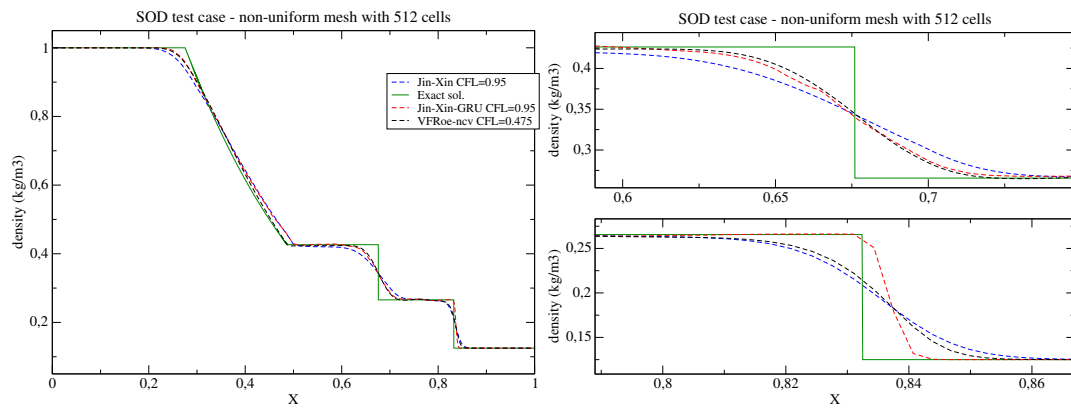


Figure 14: SOD test case: approximated density profiles for the SOD Riemann problem, the mesh is non-uniform and contains 512 cells. On the left the whole domain, on the right zoom on the contact wave (top) and on the shock wave (bottom) profiles.

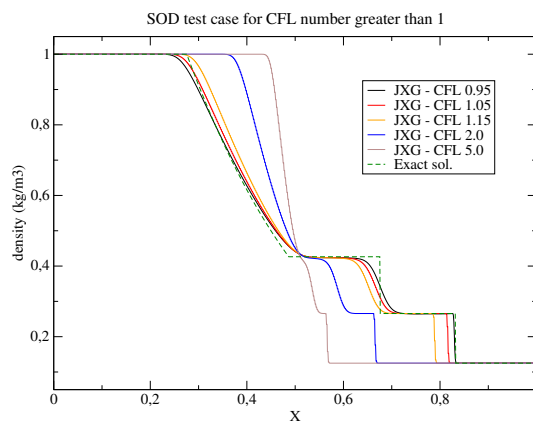


Figure 15: SOD test case: approximated density profiles for the SOD Riemann problem and CFL numbers greater than 1 with the Jin-Xin-GRU scheme. The mesh is uniform and contains 1024 cells. Approximated solutions are no more in agreement with the exact solution.

3.6 Discussion on CPU efficiency for real EOS

The results of the previous sections have been obtained by using perfect gas EOS. For this EOS, the calls to thermodynamical properties are affordable in terms of CPU-time. When using real EOS the cost of thermodynamical functions may be much higher, and it should be recalled that with approximate Riemann solvers these calls are needed at each interface and each time-step. All the schemes do not require the same amount of thermodynamical calls. For instance the VFRoe-ncv scheme using variable (U, P, s) requires 7 thermodynamical calls per interface and per time-step, while the Jin-Xin relaxation schemes with or without GRU step only require 2 thermodynamical calls. This means a ratio of 3.5 between VFRoe-ncv (U, P, s) scheme and Jin-Xin relaxation schemes.

In an asymptotic manner, when the thermodynamical calls are very costly, this ratio should be recovered in terms of the CPU-time for performing the same computation with VFRoe-ncv (U, P, s) scheme and Jin-Xin relaxation schemes. This has been checked by adding the following simple “idle” loop to every thermodynamical functions:

$$\text{for } i = 1..N_{eos}, \quad tmp = \sqrt{N_{eos}}.$$

The sole goal of this loop is to artificially increase the cost of thermodynamical calls while keeping perfect gas EOS that allows to compute easily the analytical solutions of the Riemann problems: the greater N_{eos} , the more expensive the thermodynamical calls.

With this modification, approximate solutions of the SOD problem of section 3.4 have been computed with $N_{eos} = \{25, 50, 100\}$. The case $N_{eos} = 0$ obviously corresponds to the results of section 3.1, for which (34) and (35) hold. For the case $N_{eos} = 25$ the increase of the CPU-time with respect to $N_{eos} = 0$ is equal to a factor ~ 7 which is typically the factor obtained by comparing perfect gas EOS and tabulated EOS (see [13] for instance). The results for $N_{eos} = \{25, 50, 100\}$ are given here following the notations of section 3.1:

$$\begin{aligned} \text{for } N_{eos} = 25, & \quad CPU_{vf}(\Delta x) \sim 3.35 \times CPU_{jx}(\Delta x) \quad \text{and} \quad CPU_{vf}(\Delta x) \sim 3.14 \times CPU_{jxg}(\Delta x), \\ \text{for } N_{eos} = 50, & \quad CPU_{vf}(\Delta x) \sim 3.48 \times CPU_{jx}(\Delta x) \quad \text{and} \quad CPU_{vf}(\Delta x) \sim 3.23 \times CPU_{jxg}(\Delta x), \\ \text{for } N_{eos} = 100, & \quad CPU_{vf}(\Delta x) \sim 3.49 \times CPU_{jx}(\Delta x) \quad \text{and} \quad CPU_{vf}(\Delta x) \sim 3.31 \times CPU_{jxg}(\Delta x). \end{aligned}$$

These results clearly show that the theoretical ratio 3.5 is almost recovered. The right plot in figure 9 is reproduced here by using the ratio for “real EOS”:

$$CPU_{vf}(\Delta x) \sim 3.31 \times CPU_{jxg}(\Delta x) = CPU_{jx}(\Delta x),$$

which gives $\alpha \sim 0.55$. The left plot in figure 9 obtained for perfect gas EOS is reproduced in figure 16 (left plot) together with the results obtained with $\alpha \sim 0.55$ (right plot).

It can be observed that for this test case, the Jin-Xin-GRU scheme has a little advantage over the VFRoe-ncv scheme in terms of efficiency (i.e. error with respect to CPU-time), while the VFRoe-ncv scheme remains more efficient than the Jin-Xin relaxation scheme without GRU step. Indeed, The two relaxation schemes have the same number of thermodynamical calls but the GRU step add a little cost to the Jin-Xin relaxation scheme, which explains that $CPU_{jxg}(\Delta x) \sim 1.5 \times CPU_{jx}(\Delta x)$ for $N_{eos} = 0$ (see section 3.1). When N_{eos} is increased, this difference becomes negligible and the two relaxation schemes tend to the same computational cost. Since the GRU step largely improves the accuracy of the Jin-Xin relaxation scheme, it follows that it provides a large improvement in terms of efficiency.

Aside these considerations regarding the computational efficiency, it should be recalled that we only consider here EOS (in fact perfect gas EOS) for which all schemes are robust. With realistic complex EOS, which are usually highly non-linear, many schemes may have robustness issues. This is typically the case for VFRoe-ncv schemes while relaxation schemes are known to be more robust with respect to EOS non-linearities or complexity, see [13] for instance.

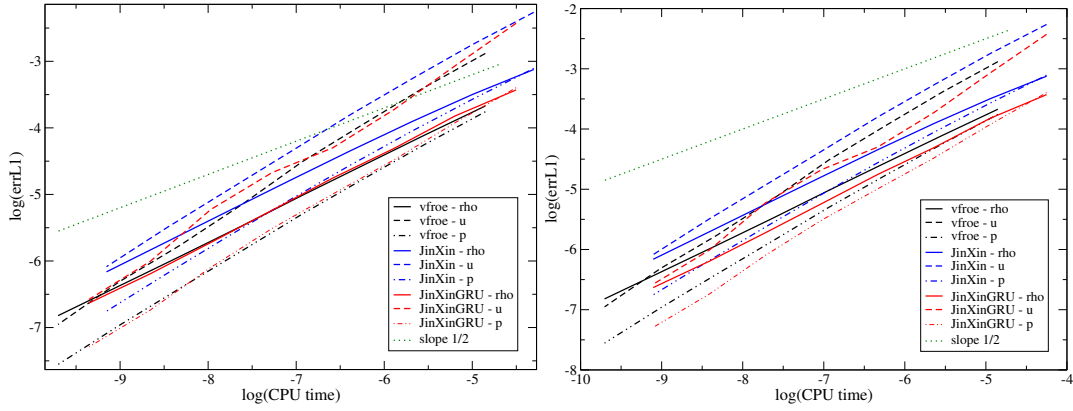


Figure 16: SOD test case: convergence curves for the three schemes with respect to the CPU-time. Perfect gas EOS results are on the left and “real EOS” results are on the right with $\alpha \sim 0.55$ for both relaxation schemes. Meshes contain from 128 up to 16384 cells.

4 Conclusion

The GRU step globally improves the accuracy of the Jin-Xin relaxation scheme. This is particularly the case for non-uniform meshes which are of prime interest for industrial applications. For the test cases with perfect gas EOS, the VFRoe-ncv scheme remains the best option regarding the Jin-Xin relaxation scheme with or without the GRU step. It is slightly different with a real EOS as shown in section 3.6. This behavior arises from two reasons.

- First, relaxation schemes are known for their ability to handle complex (real) EOS, while the VFRoe-ncv scheme may have stability issues on real EOS (see [13] for instance) as many approximate Riemann solvers.
- On the contrary to the Jin-Xin relaxation schemes, the VFRoe-ncv scheme requires numerous calls to thermodynamic properties which may be very CPU consuming with real EOS. This significantly increases the advantage of the Jin-Xin-GRU relaxation scheme over the VFRoe-ncv scheme in terms of CPU time.

Moreover, two important features of the Jin-Xin-GRU scheme are worth recalling here. Firstly, with the Jin-Xin-GRU scheme, the approximated shock waves are sharp but not located at the exact location. This is due to the loss of conservativity introduced in the GRU step. Nonetheless, it is important to note that approximated shocks converge towards the exact ones as the mesh size tends to zero. Hence, this loss of conservativity diminishes with mesh refinement. Secondly, the stochastic choice arising in the GRU step introduces some oscillations in the approximated solutions (with respect to the approximated solutions obtained with the Jin-Xin relaxation scheme). Nevertheless, the latter are stable and vanish when the mesh size tends to zero.

References

- [1] R. Abgrall and D. Torlo. High order asymptotic preserving deferred correction implicit-explicit schemes for kinetic models. *SIAM Journal on Scientific Computing*, 42(3):B816–B845, 2020.
- [2] F. Bouchut. *Nonlinear stability of finite Volume Methods for hyperbolic conservation laws: And Well-Balanced schemes for sources*. Springer Science & Business Media, 2004.
- [3] C. Chalons and J.-F. Coulombel. Relaxation approximation of the euler equations. *Journal of Mathematical Analysis and Applications*, 348(2):872–893, 2008.
- [4] A. J. Chorin. Random choice solution of hyperbolic systems. *Journal of Computational Physics*, 22(4):517–533, 1976.
- [5] P. Colella. Analysis of the effect of operator splitting and of the sampling procedure on the accuracy of glimm’s method. *Report No. LBL-8774. California Univ., Berkeley (USA). Lawrence Berkeley Lab.*, 1978.
- [6] P. Colella. Glimm’s method for gas dynamics. *SIAM Journal on Scientific and Statistical Computing*, 3(1):76–110, 1982.
- [7] F. Coquel and B. t. Perthame. Relaxation of energy and approximate riemann solvers for general pressure laws in fluid dynamics. *SIAM Journal on Numerical Analysis*, 35(6):2223–2249, 1998.
- [8] D. Coulette, E. Franck, P. Helluy, M. Mehrenberger, and L. Navoret. High-order implicit palindromic discontinuous galerkin method for kinetic-relaxation approximation. *Computers & Fluids*, 190:485–502, 2019.
- [9] F. Delarue and F. Lagoutière. Probabilistic analysis of the upwind scheme for transport equations. *Archive for rational mechanics and analysis*, 199(1):229–268, 2011.
- [10] T. Gallouët and O. Hurisse. Convergence of a multidimensional glimm-like scheme for the transport of fronts. *IMA Journal of Numerical Analysis*, 07 2021.
- [11] T. Gallouët, O. Hurisse, and S. Kokh. A random choice scheme for scalar advection. *International Journal for Numerical Methods in Fluids*, 2023.
- [12] J. Glimm. Solutions in the large for nonlinear hyperbolic systems of equations. *Communications on pure and applied mathematics*, 18(4):697–715, 1965.
- [13] P. Helluy, O. Hurisse, and L. Quibel. Assessment of numerical schemes for complex two-phase flows with real equations of state. *Computers & Fluids*, 196:104347, 2020.
- [14] O. Hurisse. On the use of glimm-like schemes for transport equations on multidimensional domain. *International Journal for Numerical Methods in Fluids*, 93(4):1235–1268, 2021.
- [15] S. Jin and Z. Xin. The relaxation schemes for systems of conservation laws in arbitrary space dimensions. *Communications on pure and applied mathematics*, 48(3):235–276, 1995.
- [16] T.-P. Liu. The deterministic version of the glimm scheme. *Communications in Mathematical Physics*, 57(2):135–148, 1977.
- [17] I. Suliciu. On the thermodynamics of fluids with relaxation and phase transitions. *Fluids with relaxation. Internat. J. Engrg. Sci*, 36:921–947, 1998.